Electronic Supplementary Material (ESI) for Photochemical & Photobiological Sciences.

Electronic Supplementary Information

Highly-performance Förster resonant energy transfer-based dye-sensitized photocatalytic H_2 evolution with graphene quantum dots as a homogenous energy donor

Yonggang Lei,‡ Yuan Xue,‡ Yanan Li, Xiangyu Liu, Fang Wang* and Shixiong Min*

School of Chemistry and Chemical Engineering, Key Laboratory of Electrochemical Energy Conversion Technology and Application, North Minzu University, Yinchuan, 750021, Ningxia Province, People's Republic of China.

*Corresponding author. E-mail: wangfang987@126.com (F. Wang); sxmin@nun.edu.cn (S. Min).

‡These authors contribute to this work equally.

Tel: 86-951-2067917; Fax: 86-951-2067915

1. Experimental

1.1 Chemicals and materials

All reagents were of analytical grade and used without further purification. TiO_2 nanoparticles (P25, 20% rutile and 80% anatase) were purchased from Degussa. Graphene oxide (GO) with lateral size of 0.2~10 μm was purchased Ashine Advanced Carbon Materials (Changzhou) Company. Graphene (Gr) nanopowder (3 nm flakes) for R&D use was kindly provided by Uniregion Bio-Tech Company. g-C_3N_4 nanosheets were prepared by pyrolyzing urea at 550 ^oC for 2 h. Deionized (DI) water was produced using YL-100B-D water purification system.

1.2 Synthesis of N, S co-doped GQDs (NSGQDs)

0.5 g of citric acid and 0.5 g of thiourea were dissolved into 20 mL of DI water under stirring. Then, the mixture solution was heated in a microwave oven (700 W) for 10 min under stirring at 450 rpm until the solution changed from colorless to dark brown, showing the carbonization of the reactant. After cooling to room temperature, 20 mL of DI water was added to dissolve the product. The as-obtained dark brown solution was centrifuged under 10000 rpm for 5 min, and then the particles were successively filtered through 0.22 μm and 25 nm filter membranes. Finally, the clear solution was concentrated with a rotary evaporator and then freeze-dried to get brown solid.

1.3 Characterization

Transmission electron microscopy (TEM) and high-resolution TEM (HRTEM) images were taken with a Tecnai-G^2-F30 field emission transmission electron microscope. X-ray diffraction (XRD) patterns were investigated with a Rigaku B/Max-RB diffractometer with a nickel filtrated Cu *K*α radiation. X-ray photoelectron spectroscopy (XPS) measurements of the samples were performed on a K-Alpha surface analysis (Thermon Scientific) using X-ray monochromatization. Fourier transform infrared spectroscopy (FTIR) spectra were performed on Thermo Nicolet Avatar 380 FT-IR spectrometer. UV–vis absorption spectra were obtained with a TU-1810 UV–vis spectrophotometer (Beijing Persee). Photoluminescence spectra were

determined by a Horiba Scientific FluoroMax-4 spectrofluorometer. The fluorescence decay times were measured using the Horiba Jobin Yvon Data Station HUB operating in time-correlated single photon counting mode (TCSPC) with the time resolution of 200 ps. Nano LED diode emitting pulses at 370 and 454 nm with 1MHz repetition rate was used as an excitation source. Light-scattering Ludox solution wasused to obtain the instrument response function (prompt). The time ranges are 0.055 ns/channel in 4096 effective channels.

1.4 Photocatalytic H_2 evolution reactions

The photocatalytic H_2 production experiments were performed in a 250 mL Pyrex reaction cell connected to a closed gas circulation and evacuation system (CEL-SPH2N, CEAULIGHT). A 300-W Xe lamp (CEL-HXF300) equipped with an optical cut-off filter ($\lambda \geqslant 420$ nm) was used as light source. In a typical experiment, a certain amounts of ErB and NSGQDs were added to a quartz reaction cell containing 100 mL of 15 vol.% TEOA aqueous solution under vigorous stirring. The pH value of the TEOA solution was adjusted by using aqueous HCl solution or diluted NaOH solution prior to reaction. To facilitate the H_2 evolution reaction, a certain volume of H_2PtCl_6 (4 mg L^{-1}) was added into above solution to form Pt nanoparticles during the photocatalytic H_2 evolution reaction. Before light irradiation, the reaction system was thoroughly degassed by evacuation in order to remove the oxygen inside. The reaction solution was continuously stirred and maintained at 304 K by a flow of cooling anhydrous ethanol during the photocatalytic reaction. The amount of evolved H_2 was analyzed using an on-line gas chromatograph (CEL-GC-7920, TCD, N_2 carrier). The apparent quantum efficiency (AQE) was measured under the same photocatalytic reaction conditions with irradiation light through a band-pass filter. The photon flux of incident light was determined using a Ray virtual radiation actinometer (Apogee MQ-500, silicon ray detector, light spectrum, 389–692 nm; measurement range, 0-4000 μmol m^{-2} s^{-1}). The apparent quantum efficiency for H_2 evolution was calculated from the ratio of the number of reacted electrons during hydrogen evolution to the number of incident photons.

2. Supplementary data

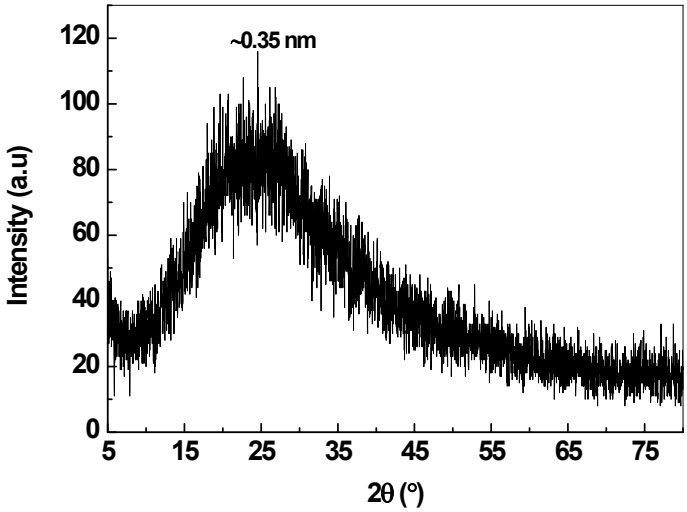

Fig. S1 XRD pattern of NSGQDs.

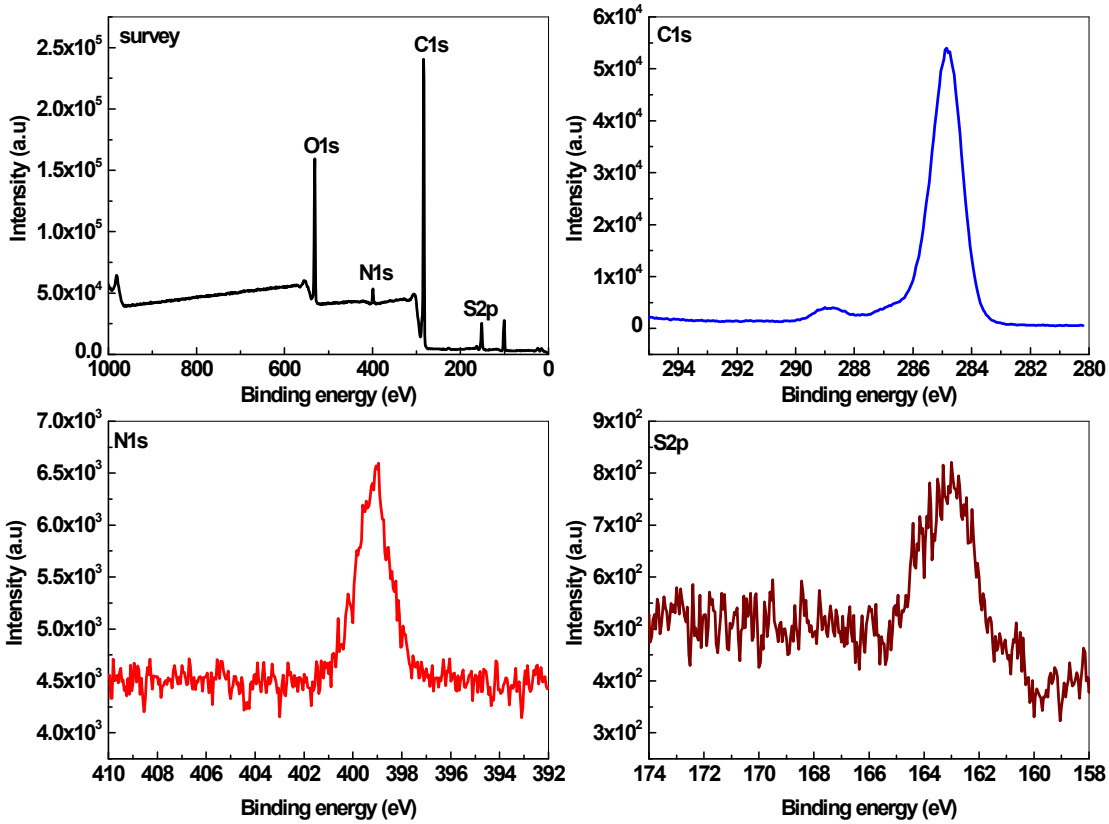

Fig. S2 Wide and high-resolution XPS spectra of C 1s, N 1s, and S 2p of NSGQD.

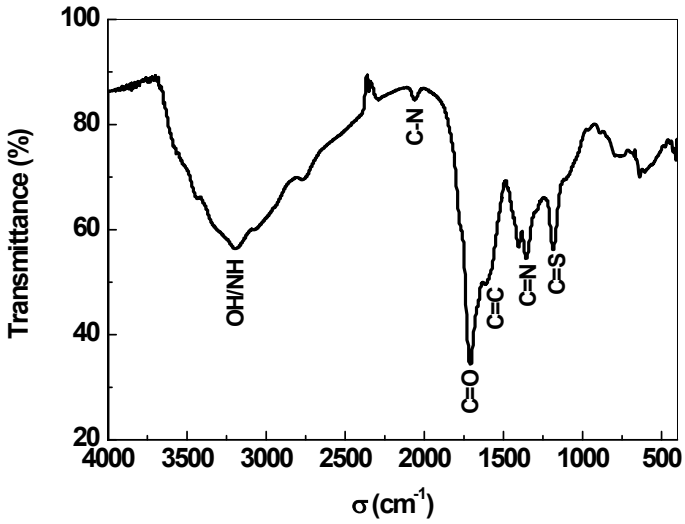

Fig. S3 FTIR spectrum of NSGQDs.

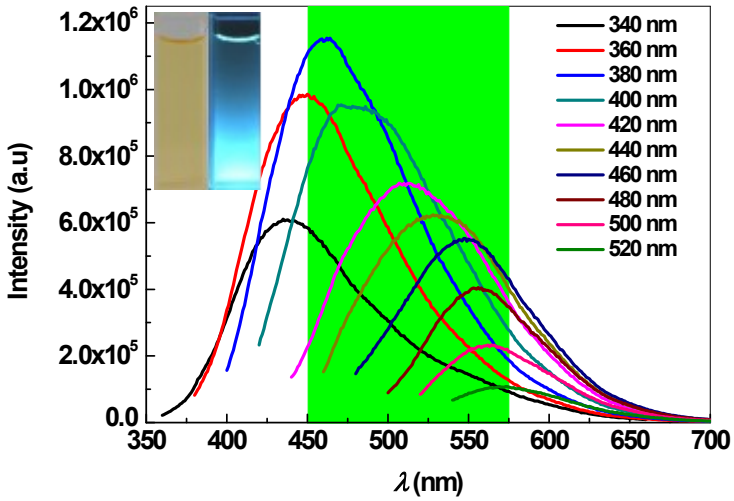

Fig. S4 Excitation-dependent PL emission spectra of NSGQDs.

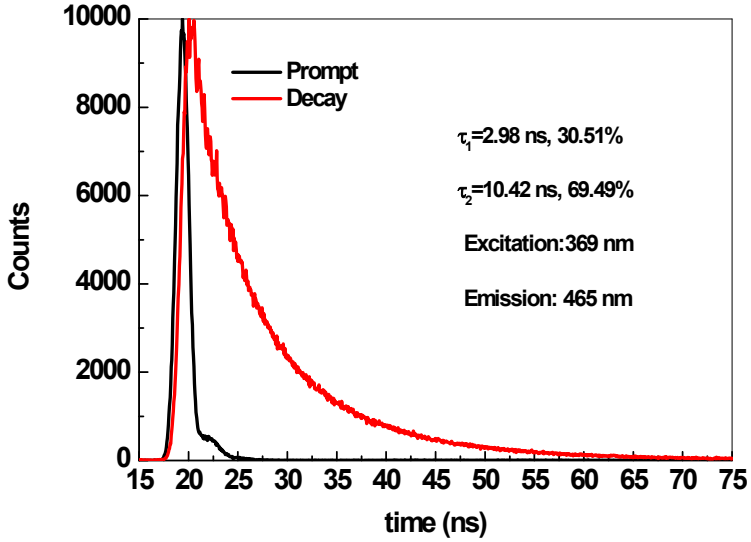

Fig. S5 Time-resolved PL spectrum of NSGQDs.

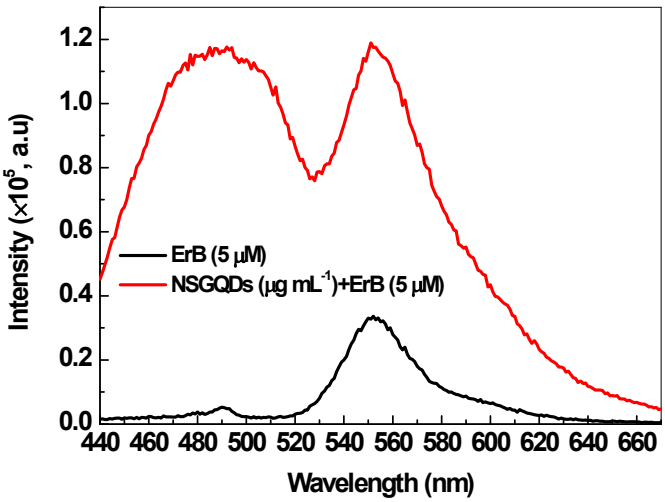

Fig. S6 Comparison of ErB emissions in the presence and absence of NSGQDs. The excitation wavelength is 420 nm with a slit of 2 nm.

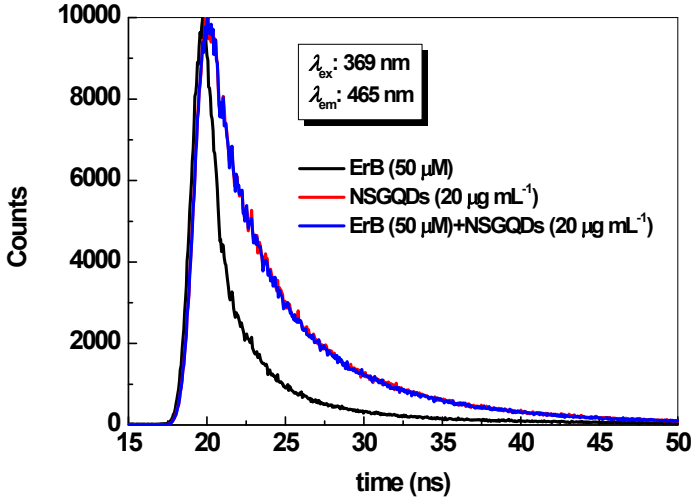

Fig. S7 PL decay profiles of ErB and NSGQDs in the absence and presence of ErB. The excitation wavelength and detection wavelength are 369 and 465 nm, respectively, with a slit of 2 nm.

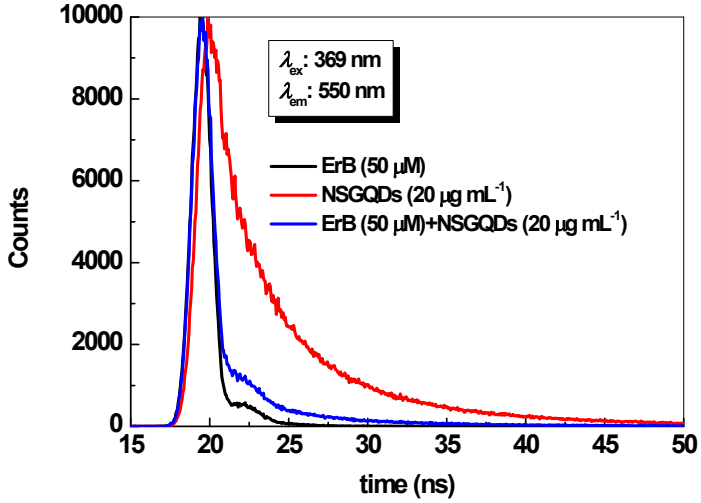

Fig. S8 PL decay profiles of NSGQDs and ErB in the absence and presence of NSGQDs. The excitation wavelength and detection wavelength are 369 and 550 nm, respectively, with a slit of 2 nm.

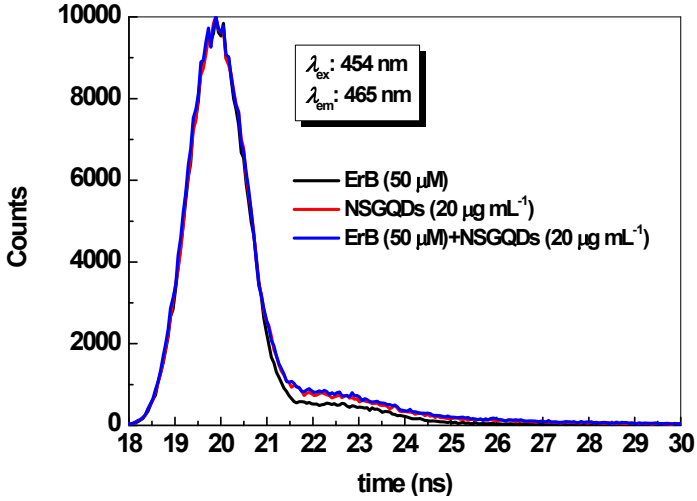

Fig. S9 PL decay profiles of ErB and NSGQDs in the absence and presence of ErB. The excitation wavelength and detection wavelength are 454 and 465 nm, respectively, with a slit of 2 nm.

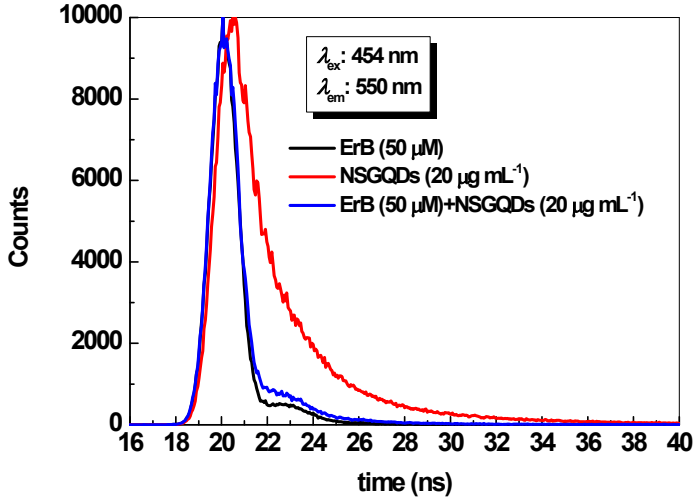

Fig. S10 PL decay profiles of NSGQDs and ErB in the absence and presence of NSGQDs,. The excitation wavelength and detection wavelength are 454 and 550 nm, respectively, with a slit of 2 nm.

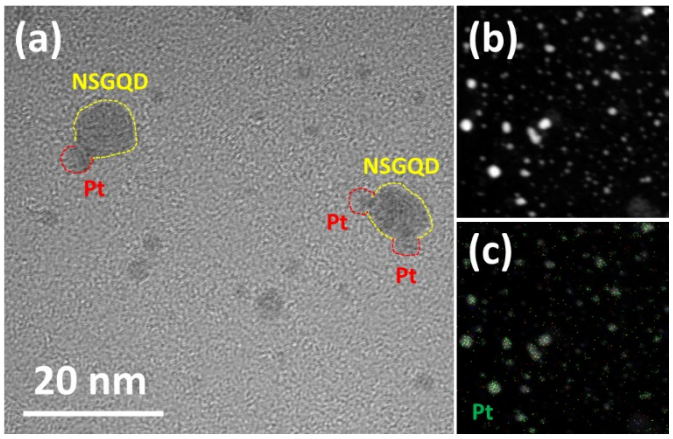

Fig. 11 (a) TEM image, (b) HAADF-STEM image, and (c) Pt element mapping of NSGQD-Pt catalyst.

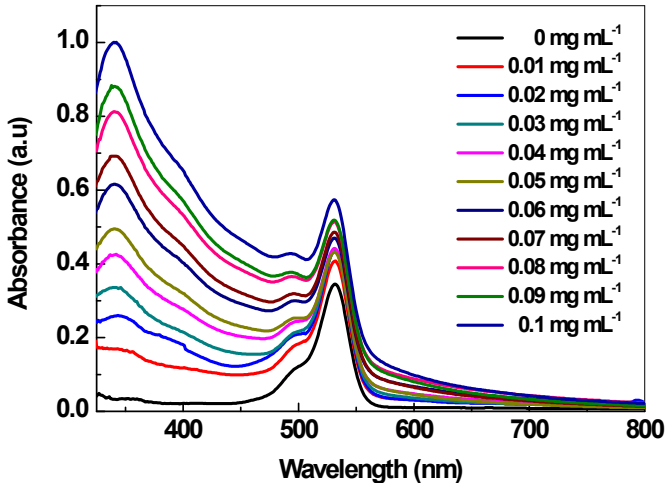

Fig. S12 UV-vis absorption spectra of ErB (5 μM) in the presence of different amounts of NSGQDs.

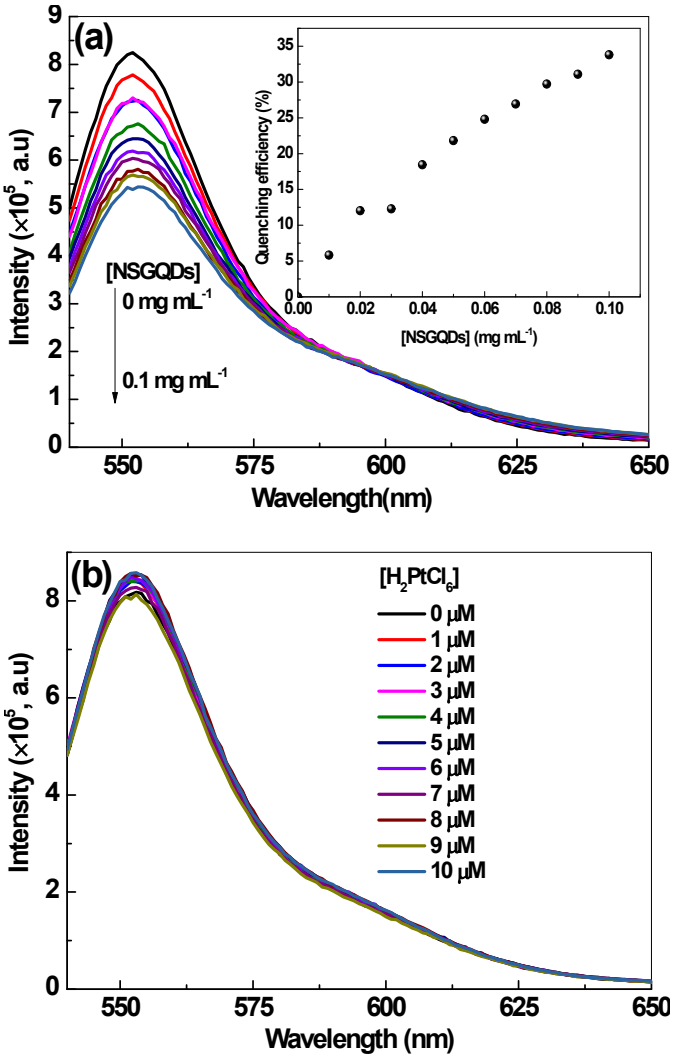

Fig. S13 PL spectra of ErB (5 μM) in the presence of different concentrations of (a) NSGQDs and (b) H_2PtCl_6. The inset in panel (a) shows the variation of quenching efficiency of ErB with concentration of NSGQDs. The excitation wavelength and slit are 520 nm and 2 nm, respectively.

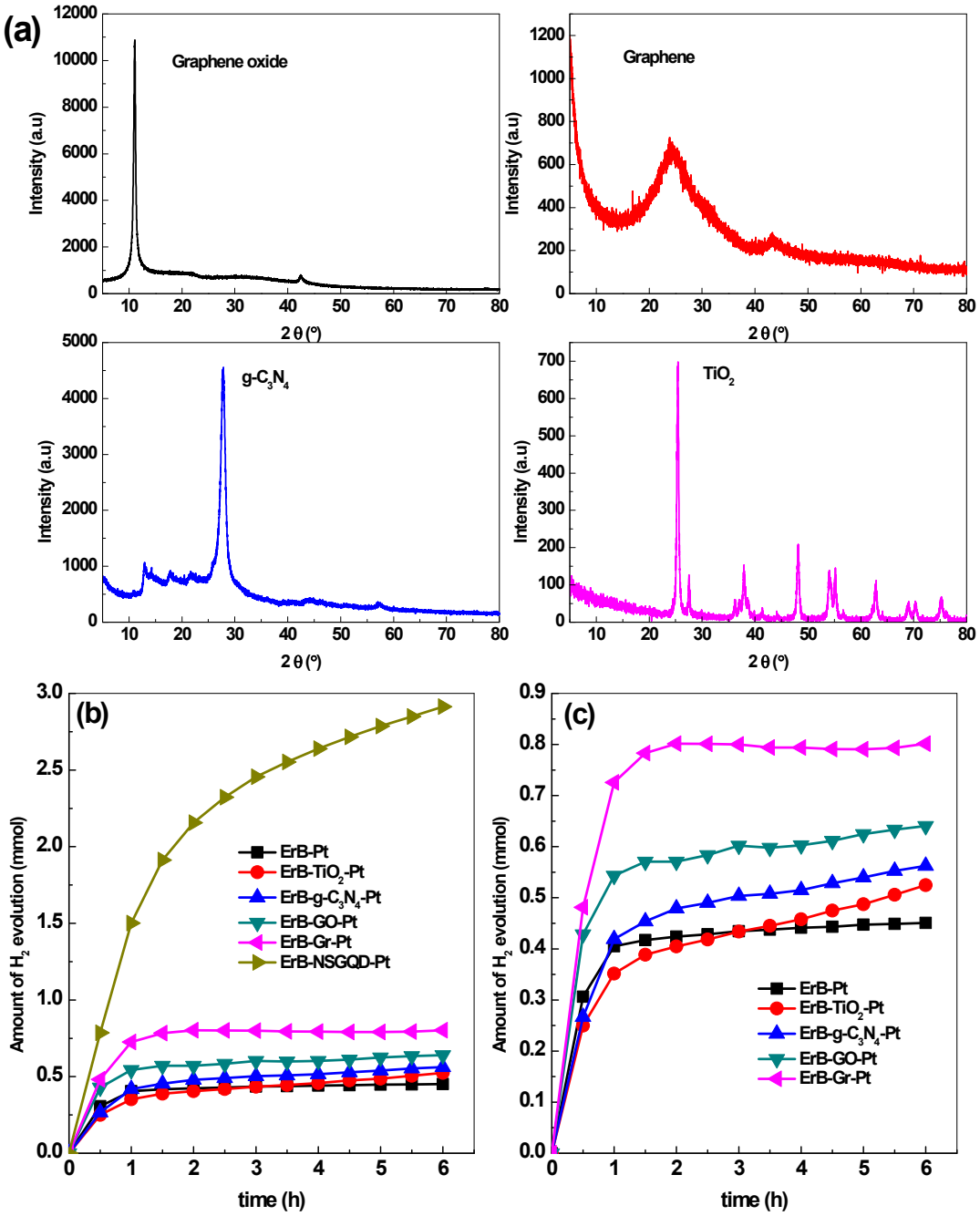

Fig. S14 (a) XRD patterns of graphene oxide (GO), graphene (Gr), g-C_3N_4, and TiO_2. (b, c) Comparison of H_2 evolution from ErB sensitized system in the presence of NSGQDs, TiO_2, g-C_3N_4, GO, and Gr. Conditions: ErB, 0.5 mM; NSGQDs, TiO_2, g-C_3N_4, GO, or Gr, 10 mg; Pt, 100 μM; TEOA, 100 mL (15%, pH 8); light source, Xe lamp (300 W), ≥420 nm.

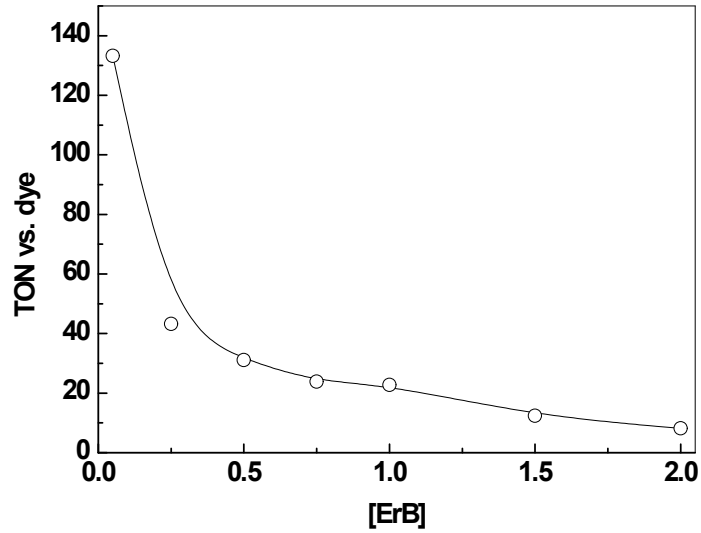

Fig. S15 The dependence of total turnover numbers of H_2 evolution from ErB-NSGQD-Pt system on ErB concentration. Reaction conditions: NSGQDs, 10 mg; Pt, 25 μM; TEOA solution, 100 mL (15%, pH 8); light source, Xe lamp (300 W), ≥420 nm.

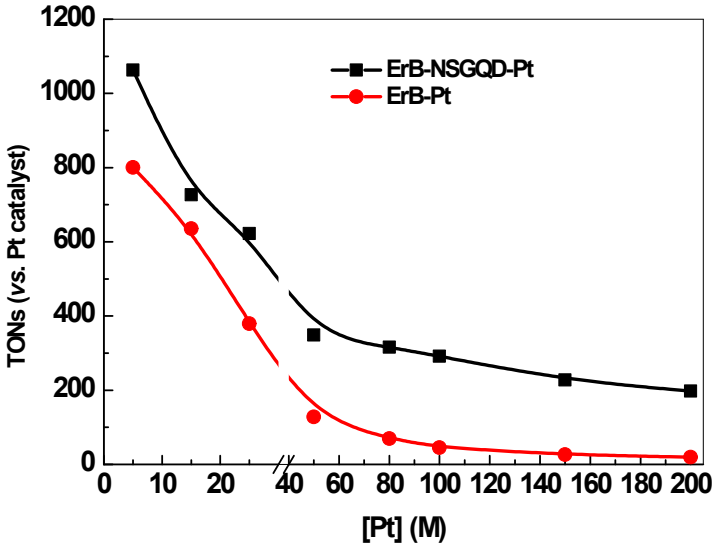

Fig. S16 The dependence of total turnover numbers of H_2 evolution from ErB-NSGQD-Pt and ErB-Pt systems on Pt concentration. Reaction conditions: NSGQDs, 10 mg; ErB, 0.5 mM; TEOA, 100 mL (15%, pH 8); light source, Xe lamp (300 W), ≥420 nm.

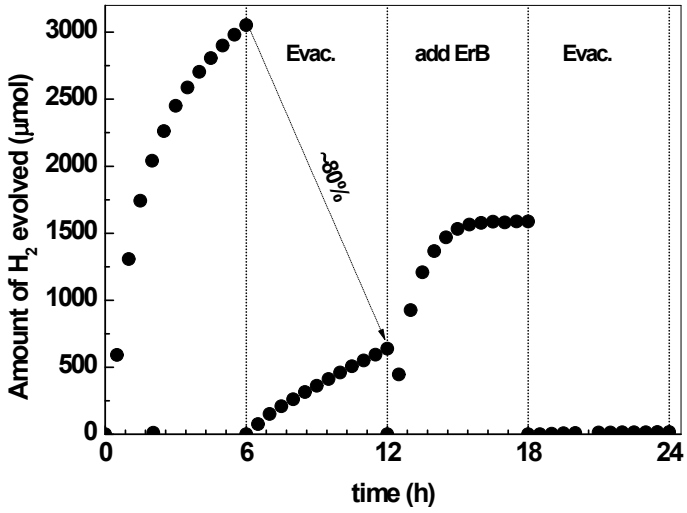

Fig. S17 H_2 production in the recycle study over the ErB-NSGQD-Pt (ErB, 0.5 mM; NSGQDs, 10 mg; Pt, 100 μM). Conditions: TEOA, 100 mL (15%, pH 8); light source, Xe lamp (300 W), ≥420 nm.